Pacific Northwest
NATIONAL LABORATORY

PNNL-34758

How a Large-Scale Deployment of Grid-Forming Inverters May Impact Inter-Area Oscillation Modes

An Investigation in the US Western Interconnection

August 31, 2023

Shuchismita Biswas
Quan Nguyen
Xue Lyu
Xiaoyuan Fan
Wei Du
Jim Follum
Zhenyu Huang

U.S. DEPARTMENT OF ENERGY
Prepared for the U.S. Department of Energy
Under contract DE-AC05-76RL01830

PACIFIC NORTHWEST NATIONAL LABORATORY
operated by
BATTELLE
for the
UNITED STATES DEPARTMENT OF ENERGY
under Contract DE-AC05-76RL01830

Printed in the United States of America

Available to DOE and DOE contractors from
the Office of Scientific and Technical
Information,
P.O. Box 62, Oak Ridge, TN 37831-0062
www.osti.gov
ph: (865) 576-8401
fox: (865) 576-5728
email: reports@osti.gov

Available to the public from the National Technical Information Service
5301 Shawnee Rd., Alexandria, VA 22312
ph: (800) 553-NTIS (6847)
or (703) 605-6000
email: info@ntis.gov
Online ordering: http://www.ntis.gov

PNNL-34758

How a Large-Scale Deployment of Grid-Forming Inverters May Impact Inter-Area Oscillation Modes

An Investigation in the US Western Interconnection

August 31, 2023

Shuchismita Biswas
Quan Nguyen
Xue Lyu
Xiaoyuan Fan
Wei Du
Jim Follum
Zhenyu Huang

Prepared for
the U.S. Department of Energy
Under Contract DE-AC05-76RL01830
Pacific Northwest National Laboratory
Richland, Washington 99352

Abstract

This report describes work performed to evaluate the impact of high grid-forming (GFM) inverter penetration on the inter-area oscillation mode characteristics of the Western Interconnection. Particularly, this work uses simulations to analyze how: a) replacing fossil-fuel-based synchronous generators by GFM inverters will impact properties of the inter-area modes that see heavy participation from hydropower generators in the northwestern WI, and b) replacing the Colstrip power plant by grid-following (GFL) and GFM inverters will change the characteristics of the Montana mode. Results obtained indicate that high penetration of GFM inverters will significantly alter inter-area oscillation characteristics in interconnections. Low frequency oscillations in the 0.1-1 Hz range will be predominantly driven by synchronous machines, and hence their relative distribution in the interconnection will impact mode characteristics and observability.

Acknowledgments

The project team at PNNL would like to acknowledge funding support from the U.S. DOE Office of Electricity Advanced Grid Modeling (AGM) program, and continuous feedback and comments from the project technical advisors.

In addition, the project team is grateful to Dr. Dan Trudnowski of Montana Tech and our PNNL colleagues, particularly Dr. Pavel Etingov, Dr. Kaustav Chatterjee, and Dr. Yousu Chen, for their support, review, and feedback for this work.

Acronyms and Abbreviations

BC British Columbia

COI California-Oregon Intertie

EMT Electromagnetic transient

GFL Grid-Following

GFM Grid-Forming

IBR Inverter-based Resource

MVS Modeling and Validation Subcommittee

MT Montana

NS North-South

PCC Point of Common Coupling

PI Proportional-Integral

PLL Phase-Locked Loop

PMU Phasor Measurement Unit

SSAT Small Signal Analysis Tool

WECC Western Electricity Coordinating Council

WI Western Interconnection

Contents

Figures

Tables

1.0 Introduction

Low-frequency inter-area oscillations, typically between 0.1 and 1 Hz, appear in a power system due to the electromechanical energy exchange among groups of generators located in distant parts of an electrical interconnection. Inter-area oscillation modes are characteristic properties of an electric interconnection and can be described by their frequency, damping ratio (DR), and shape [1]. Poorly damped oscillation modes may pose stability concerns and hence are monitored closely by system operators. Moreover, as inverter-based renewable energy resources gradually displace fossil-fuel-based synchronous generators to facilitate grid decarbonization, the characteristics of existing dominant system modes are expected to change. It is essential to understand what changes may occur and identify potential stability concerns before they morph into serious reliability threats.

Previous research has shown that the properties of inter-area modes are influenced by several factors like system load, network topology, power flow patterns, and inverter-based resource (IBR) penetration. Several works in existing literature have sought to understand how increasing IBR penetration will impact system modes in different real interconnections. These works include both model-based [2–5] and measurement-based [5–7] studies. Measurement-based analyses allow investigating how heterogeneous IBR fleets with diverse capacities and control methodologies interact with synchronous machines to impact oscillation characteristics, but separating the effect of coexisting factors is challenging. Moreover, given the limited IBR penetration in today's grids, conclusions drawn from field measurements may not be directly extrapolated to IBR-dominated future grids. On the other hand, model-based approaches facilitate the examination of hypothetical scenarios and the impact of individual explanatory variables on modal properties, thereby complementing measurement-based work.

Prior model-based research has concluded that mode frequencies tend to increase with increasing IBR penetration, while DR values change only if inverters displace significant proportions of synchronous machines in areas with high participation in a mode [3, 4, 8]. Depending on IBR location, DR may either increase [3] or decrease [2, 4]. IBRs are not expected to significantly participate in inter-area electromechanical modes. Rather, controller interactions may drive local oscillation modes at higher frequencies. Moreover, as inverter controls have a wide timescale, they can also inject forced oscillations at different frequencies that may interact with inter-area modes and propagate throughout an interconnection [9]. Instances of subsynchronous oscillations visible throughout the transmission network of small island systems have also been reported recently [10].

The existing literature has not adequately explored how high penetration of grid-forming (GFM) inverters will impact natural modes of oscillation in large electric interconnections. GFM control is gaining acceptance in the industry as a promising technology for achieving high renewable energy penetration in power systems, and properly tuned GFM IBRs offer the additional advantage of quickly damping transient oscillations following system disturbances [11]. Hence, participation in low-frequency inter-area modes may not be observable at GFM inverter locations, and in high-penetration scenarios, these resources may significantly alter the frequency response of interconnections. To address this gap, this work studies the impact of replacing fossil-fuel-based synchronous machines with droop-control-based GFM inverters [12] on inter-area oscillations in the U.S. Western Interconnection (WI).

It must be noted here that the hypothetical scenarios studied in this report assume that retiring synchronous generators are replaced by droop-control-based grid-forming inverter-interfaced generators with equal power outputs. However, future IBR-dominated grids are expected to use a heterogeneous mix of GFL and GFM technologies with different control schemes such as droop-control, virtual synchronous control, and virtual oscillator control. Hence, although the studied scenarios may not accurately capture the IBR-transition, they enable the detailed examination of

Table 1. Characteristics of WI inter-area oscillation modes [5]

Mode	Frequency (Hz)	Shape
NS-A	0.2-0.3	Alberta vs. system
NS-B	0.35-0.45	Alberta vs. (northern U.S. + B.C.) vs. southern U.S.
EW-A	0.35-0.45	(Colorado + eastern Wyoming) vs. system
BC-A	0.5-0.72	Not well-understood
BC-B	0.6-0.72	Not well-understood
MT	0.7-0.9	Montana vs. system

GFM inverters' impact on wide-area oscillations. A subset of results presented in this report has been submitted to a conference [13].

1.1 Inter-area modes in the Western Interconnection

Following the WI blackout in August 1996 caused by undamped oscillations [14], much effort has been invested in understanding the properties of its inter-area modes, using both simulation-based studies and synchrophasor measurements. A recently released report by the Western Electricity Coordinating Council (WECC) documents the existing understanding of the WI modes that can be observed in system measurements, as well as their excitability, observability and controllability [5]. The frequencies and shapes of modes discussed in [5] are summarized in Table 1.

The two north-south (NS) modes are the best-understood WI modes. The NS-A mode is well-damped, with DR values greater than 10% when the 500 kV intertie between Alberta and British Columbia (BC) is in service. When Alberta disconnects from the rest of the WI, the NS-A mode disappears. The NS-B mode is the most geographically widespread and lightly damped mode in the WI, with typical DR values ranging between 5 and 10%. When the Alberta-BC intertie is disconnected, the frequency and DR of the NS-B mode are reduced. Measurement-based correlation analysis shows that system load, IBR penetration and power flow on the California-Oregon Intertie (COI) also influence the NS mode properties [6]. Due to its wide visibility and low damping, the NS-B mode is carefully monitored by grid operators in the WI.

The east-west (EW)-A and NS-B modes have overlapping frequency ranges, but can be differentiated based on their shapes. Model-based studies find preliminary evidence for two modes (BC-A and BC-B) primarily driven by large generators in BC swinging against the northern US, but due to limited PMU coverage, further research is needed to better understand their properties. The Montana (MT) mode is well-damped (DR ~ 10%) and is primarily driven by a large coal generation facility in Colstrip, MT, whose retirement is expected to impact this mode's properties significantly. This report studies how- a) a system-wide increase in GFM inverter penetration impacts the N-S and BC modes that are known to have high participation from hydropower generators clustered in the northwestern WI, and b) replacing the Colstrip synchronous machines with IBRs impacts the MT mode behavior.

1.2 Data-driven Oscillation Analysis

Due to the underlying electromechanical physics, synchronous power systems inherently are multimodal under-damped systems. A power system has multiple natural modes of oscillation, most of which tend to be localized to a few generators. Some modes, however, become widespread and involve a self-organized group of generators swinging against other self-organized generator groups in other parts of the system. These modes are termed ‘inter-area’ and typically have frequencies between 0.1 to 1 Hz. During high system stress conditions (component outages, high power transfers across corridors, etc.), inter-area oscillations may become undamped, thereby increasing the risk of outages.

Oscillation modes are typically described by their frequency, DR, and shape. Damping is a measure of how fast a given mode dissipates in a transient. A mode is considered well-damped if its DR is above 10%. The shape of a mode describes its observability. Mode shape is a complex number whose amplitude describes the relative participation of different machines in modal oscillations; and angle describes the relative grouping of generators participating in the given mode. Generators with similar mode shape angles swing together against other generator groups whose angles are about 180 degrees apart.

Analysis techniques used to estimate the properties of a given mode can be broadly grouped into three categories: a) ambient analysis [15, 16], b) ringdown analysis [17, 18], and c) eigenvalue analysis [19]. Ambient methods use phasor measurement unit (PMU) data to estimate mode properties during steady-state conditions, when the primary excitation to the power system is provided by random load changes. Ringdown methods analyze natural oscillations following a large disturbance to estimate modal content, usually by employing curve-fitting techniques. Ringdown techniques can be employed for both field PMU measurements and simulation observations. Eigenvalue analysis methods seek to estimate modes by constructing a linearized model of the system from the mathematical description of its dynamics. These methods can be implemented using offline powerflow cases with associated dynamic data of system generators, but are computationally expensive for large interconnections. Commercial tools like Small Signal Analysis Tool (SSAT) can be used for these studies [20]. For further discussion about power systems oscillations, their properties and analysis techniques, one can refer [1, 5].

Given the computational burden of eigen-analysis methods, this work has used ringdown analysis, specifically multichannel Prony analysis, to estimate WI modal properties under different IBR-penetration scenarios [17]. Other ringdown analysis methods include matrix-pencil [18, 21], dynamic mode decomposition [5] etc. Prony methods express the post-disturbance “free-response” system output as a linear combination of damped sinusoids. In this work, transient disturbances were created by simulating 1200 MW dynamic brake insertions at different locations in the network. Brake insertions at different locations may excite different inter-area modes. It is assumed that the trajectory of the modeled state follows an autoregressive process. Results obtained are sensitive to several parameters that must be user-specified (model order, data window to be analyzed). Despite this, due to the relative ease of implementation, Prony methods are useful in estimating and comparing trends in mode properties when many model-based scenarios are to be examined.

1.3 Grid-Following and Grid-Forming Inverters

In this section, the control methodologies of the GFL and GFM inverters used in this study have been described. The control strategies for inverters can be categorized into two main types: grid following (GFL) control and grid-forming (GFM) control. The GFL control strategy is extensively employed by present inverters. It controls the inverter as a current source and necessitates the

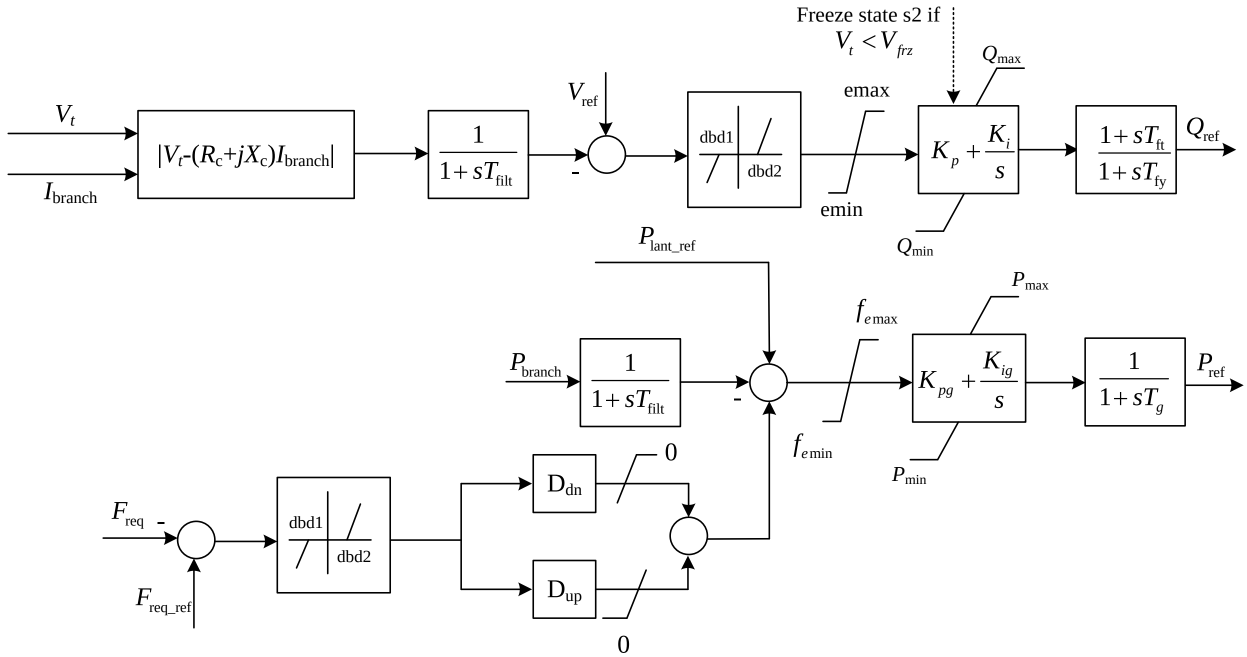

Figure 1. Generic Renewable Plant Control Model repc_a

use of a phase-locked loop (PLL) to measure the phase angle at the point of common coupling (PCC) to achieve synchronization. As renewable energy penetration increases in future power grids, the voltage at the PCC may no longer be effectively regulated solely by the remaining synchronous machines. This can lead to the inability to achieve the control objective of GFL control. To tackle this challenge, the concept of GFM control has emerged. GFM control treats the inverter as a voltage source and doesn't depend on a PLL for synchronization.

The GFL inverter is represented by *repc_a* + *reec_a* + *regc_a* in this study, and their control structures are depicted in Fig. 1, Fig. 2, and Fig. 3 respectively [22–24]. At the plant control level, both voltage control and frequency regulation are enabled. The difference between the voltage reference V_{ref} and the measured voltage, considering line droop compensation, is input into a proportional-integral (PI) controller. This controller then adjusts the output reactive power of the inverter accordingly. Additionally, the difference between the measured frequency and the frequency reference $F_{\text{req\_ref}}$ is directed to a proportional controller, which modifies the active power output of the inverter. The active and reactive power references produced at the plant control level are transmitted to the electrical control model to generate the commands of active and reactive currents of the inverter. Our control approach assigns a higher priority to regulating the reactive current. The active and reactive current commands are sent to the generator model to control the active and reactive current injected from the inverter. With this control method, the inverter is controlled as a current source.

Droop control serves as the predominant approach for GFM inverters. The synchronization process is accomplished by monitoring the power imbalance, drawing inspiration from the conventional $P-\omega$ control mechanism of a synchronous machine. It can achieve self-synchronization while using local measurements. A direct droop GFM control strategy is adopted in this study, as illustrated in Fig. 4. The frequency ω and voltage magnitude E of the inverter can be given

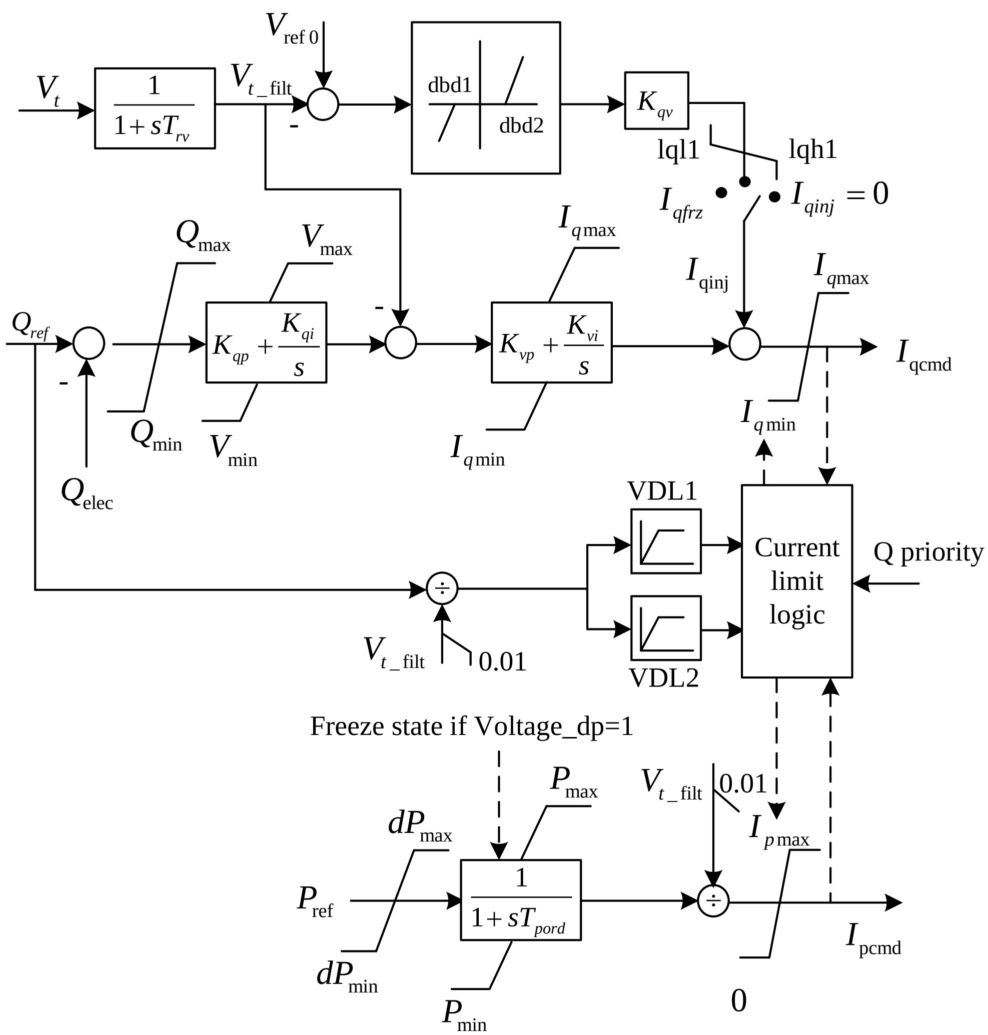

Figure 2. Generic Renewable Electrical Control Model reec_a

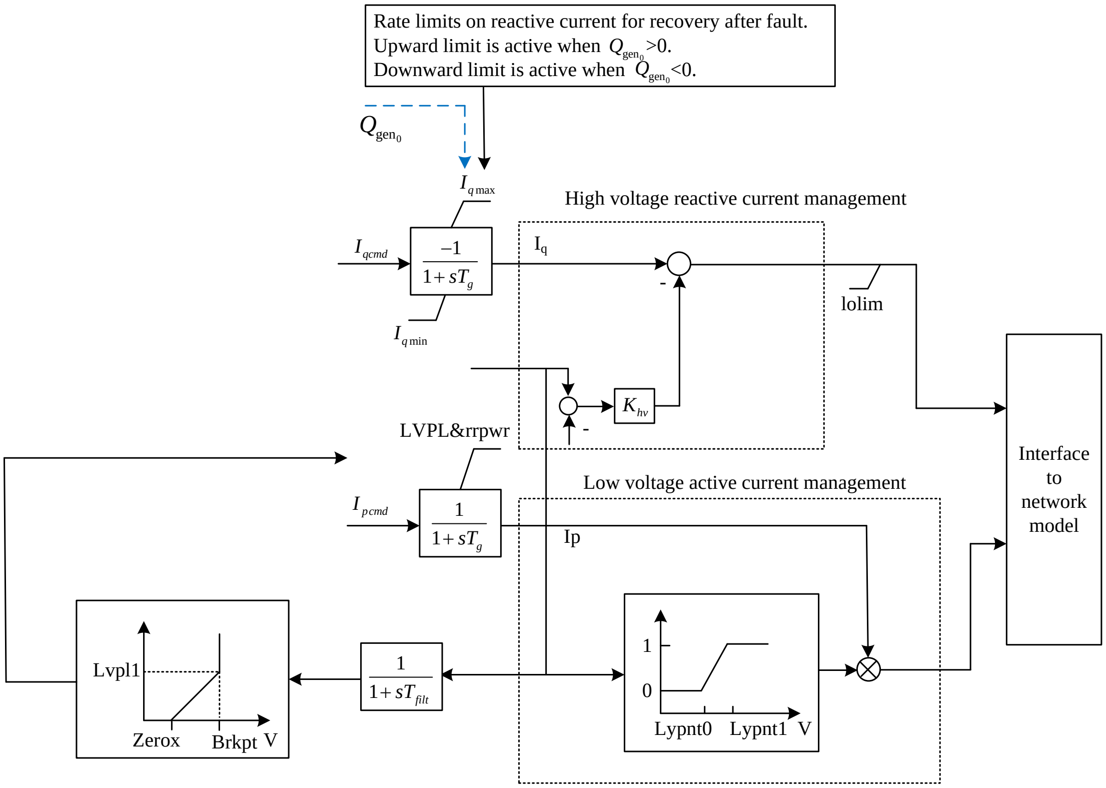

Figure 3. Generic Energy Generator Model regc_a

by,

$$\omega = \omega_0 + \frac{1}{m_p} \frac{\omega_z}{\omega_z + s}(P_{set} - P_f) \tag{1}$$

$$E = V_{set} + \frac{1}{m_q} \frac{\omega_z}{\omega_z + s}(Q_{set} - Q_f). \tag{2}$$

Here, m_p and m_q are droop coefficients; P_{set}, Q_{set} are active and reactive power references (we assume $Q_{set} = 0$); P_f, Q_f are the measured active and reactive power after the filter; and $\frac{\omega_z}{\omega_z+s}$ represents the low-pass filter applied to the power measurements.

PNNL has developed an equivalent positive sequence model for the aforementioned direct droop control based GFM inverter [25]. Within this positive sequence model, the low-pass filter, $P-f$ droop, and $Q-V$ droop control mechanisms are characterized similarly to the model utilized in the EMT simulation tool. Additionally, an active and reactive power limiting control is integrated into this positive sequence model. Specifications for this model has been approved by the WECC Modeling and Validation Subcommittee (MVS) for use in initial studies aimed at evaluating the impact of IBR integration in transmission systems. The model has been recently approved by WECC MVS, renamed as *REGFM_A1*, and is being implemented in popular simulation softwares.

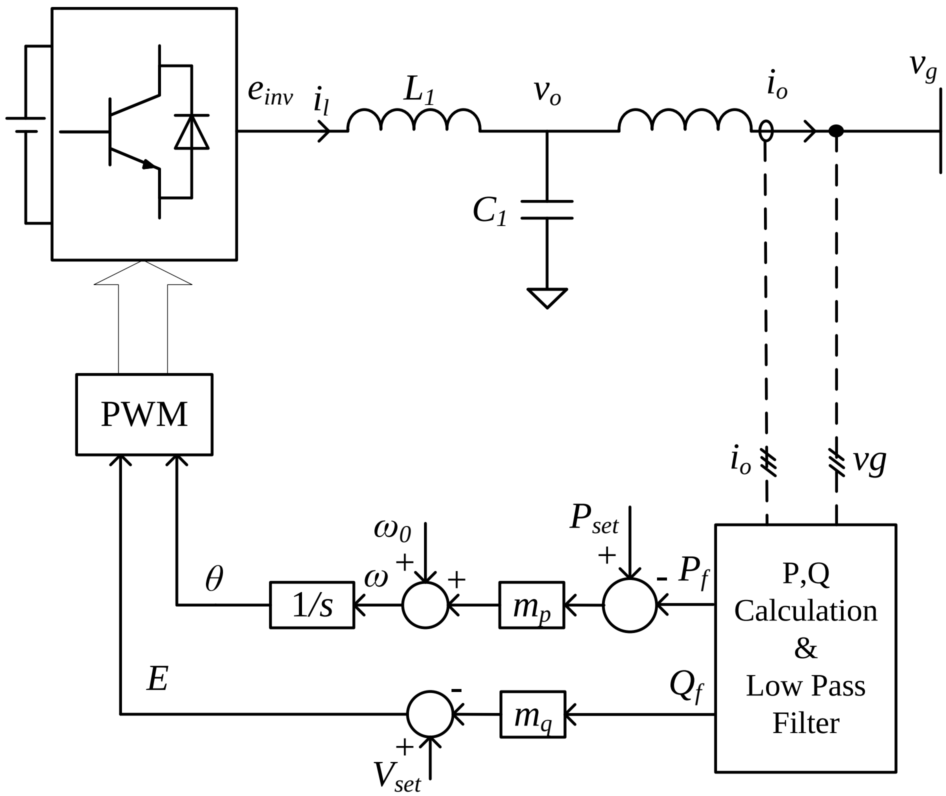

Figure 4. Direct droop GFM control utilized by REGFM_A1

2.0 Observations for Modes with High Participation from Hydropower Generators

Inter-area modes of oscillation are characteristic properties of an interconnection and are primarily driven by the electromechanical energy exchange among synchronous machines. Hence, when conventional fossil fuel generators are retired and replaced by GFM IBRs, dominant modes observed in baseline cases may shift or disappear, and new modes may emerge based on the interaction among the generators remaining in the system. In the WI, large synchronous generators that do not use fossil fuels (i.e. hydropower) are geographically clustered in British Columbia (BC) and the northwestern US with some presence along the California coast. This chapter studies how oscillations characterized by high participation of these large hydro-generators evolve following the retirement of other fossil fuel generators under different inverter penetration scenarios. At present, these are the NS-B and BC modes which may be excited by the Chief Joseph dynamic brake insertion.

The results presented are preliminary, dependent on modeling assumptions, and may not accurately capture how future IBR penetration unfolds in the WI. However, they indicate that under high-penetration scenarios, GFM inverters may significantly alter inter-area oscillations and hence, system operators must closely monitor these changes as the resource-mix continues to evolve.

2.1 Case Studies

The simulation-based studies in this work have been performed using the WECC 2031 heavy winter planning case (henceforth referred to as the base case) in PSS/E. This baseline model has about 160 GW generation, with ~ 12.5% contribution from inverter-based renewable resources (solar, wind, battery storage) and ~ 33% from hydropower, as shown in Fig. 5. Generator data from the WECC Anchor Data Set has been leveraged for scenario creation [26].

As mentioned before, ringdown analysis methods estimate modal properties from the post-disturbance trajectories of power system variables. In this work, the disturbance was created by simulating the insertion of the Chief Joseph dynamic braking resistor for 0.5 seconds to reflect real-world system tests [5,27]. The Chief Joseph brake insertion is known to excite modes where high participation from the hydrogenerators in the Northwest are observed, namely the NS-B and BC modes. Other model-based studies have also simulated brake insertions at various additional locations to study other inter-area modes in detail [4, 5].

2.2 Grid Forming Inverter Model

To simulate different GFM inverter penetration scenarios, synchronous generators in the base case were incrementally replaced by GFM IBRs with single-loop droop-based control. It is assumed that all renewable energy resources withing the plant have been integrated into a single GFM inverter. This modelling approach implies that intra-plant dynamics cannot be captured in this study. However, as this study aims to only study wide-area oscillations, intra-plant dynamics are not in scope.

The control diagram of the droop-based GFM IBRs is the same as that shown in Fig. 4. The GFM model used here has been approved for initial studies by the WECC MVS for initial studies about IBR penetration in bulk power systems. A detailed control diagram is also shown in Fig. 6. In the simulated scenarios, the aggregated IBRs had equal generation injections as the

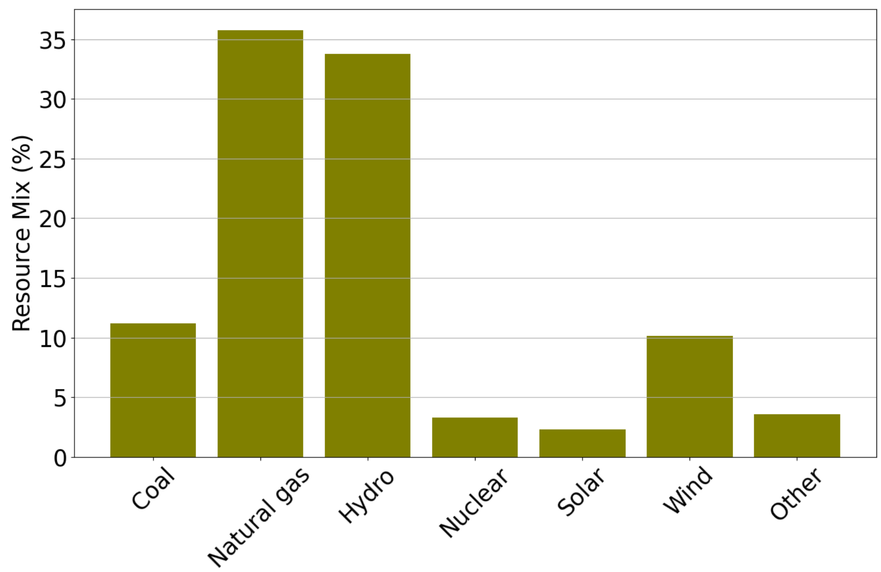

Figure 5. Generation resource mix in the WECC 2030 heavy winter planning case

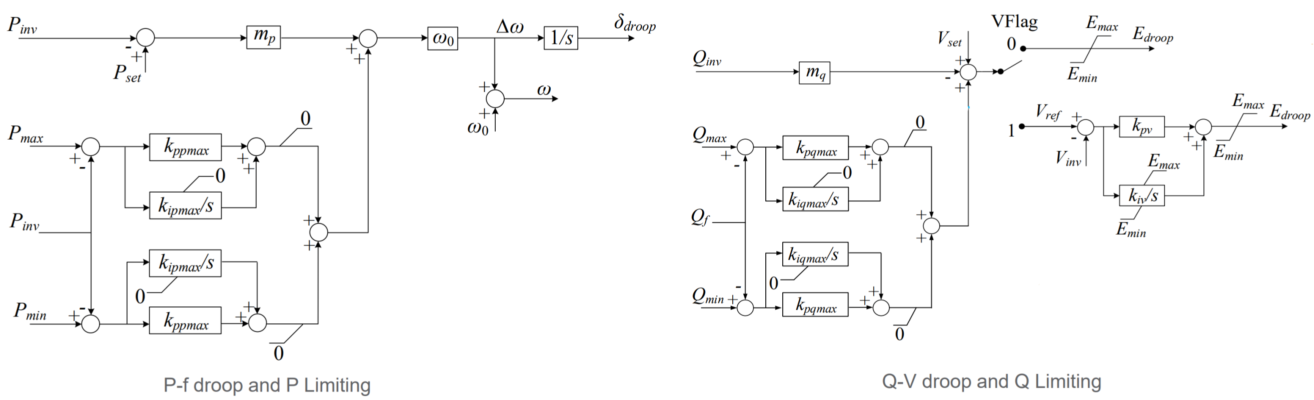

Figure 6. Droop control implemented in the REGFM_A1 model used in this work

synchronous generators being replaced, as further elaborated in subsequent sections. Existing IBRs in the base case using grid-following (GFL) controls were also replaced by GFM inverters.

A GFM inverter is modeled as a controllable voltage source behind a coupling impedance, and the droop controller controls the inverter's internal voltage magnitude and angular frequency. The positive-sequence phasor model of single-loop droop-controlled GFM inverters approved by the WECC MVS for evaluating the impact of IBR integration in transmission systems has been used here [12]. The model additionally comprises a fault current limiting function that limits the inverter current output during short-circuit conditions [25]. Model parameter values used in this work are listed in Table 2.

Automation scripts have been developed to facilitate the replacement of specified synchronous generators by GFM inverters in large PSSE powerflow cases [28]. This will ensure that the methodology used in this work can be scaled to many IBR penetration scenarios with relative ease.

Parameter	Description	Value
X_L	Inverter coupling reactance	0.15 pu
m_q	$Q-V$ droop gain	0.05 pu
k_{pv}	Proportional gain of voltage controller	0 pu
k_{iv}	Integral gain of voltage controller	5.86 pu/s
m_p	$P-f$ droop gain	0.01 pu
k_{ppmax}	Proportional gain of the overload mitigation controller	0.01 pu
k_{ipmax}	Integral gain of the overload mitigation controller	0.1 pu/s
T_{Pf}	Time constant of low-pass filter for P measurement	0.01 s
T_{Qf}	Time constant of low-pass filter for Q measurement	0.01 s
T_{Vf}	Time constant of low-pass filter for V measurement	0.01 s
k_{pqmax}	Proportional gain of the Q_{max} and Q_{min} controller	3 pu
k_{iqmax}	Integral gain of the Q_{max} and Q_{min} controller	20 pu/s
I_{max}	Inverter maximum output current	1.2 pu

Table 2. Model parameters used for GFM inverters

2.3 Scenario Creation

Three different scenarios with varying fuel mixes and resultant levels of GFM penetration were created, as summarized in Table 3. To ensure the scalability of the developed approaches and streamline future studies, a suit of automation scripts have been developed for replacing specified synchronous machines by inverters in PSS/E models of large interconnections. A visual summary of the automation process is shown in Fig. 7.

To facilitate grid decarbonization, many US states have announced ambitious plans of retiring fossil fuel fleets and replacing them with renewable sources of power. In line with these goals, while creating hypothetical scenarios of increased renewables penetration throughout the WI, synchronous generators using clean fuel sources like hydropower and geothermal generators were not replaced. In the WI, large hydropower generators are concentrated in its northwestern

Scenario	Description	GFM Penetration
1	Existing GFL inverters and coal generators in base case replaced by GFM	$\sim 23\%$
2	50% of natural gas generation in each balancing area also replaced by GFM	$\sim 46\%$
3	All natural gas and nuclear generators also replaced by GFM	$\sim 62\%$

Table 3. Creating scenarios with varying levels of GFM IBR penetration in the WI

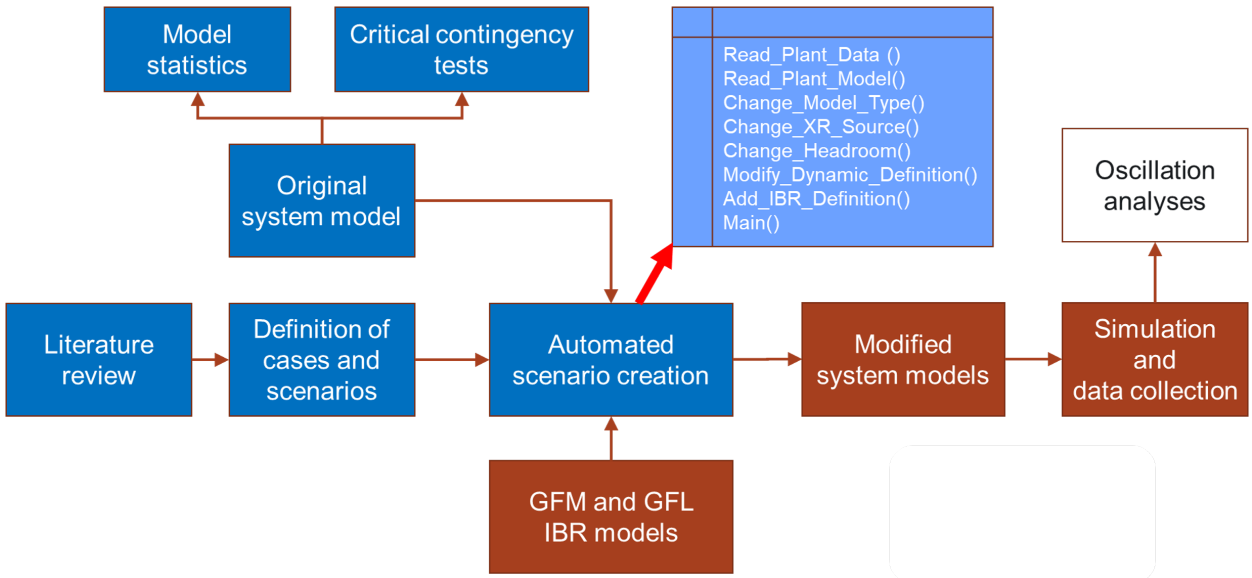

Figure 7. Structure of the automated scenario creation process

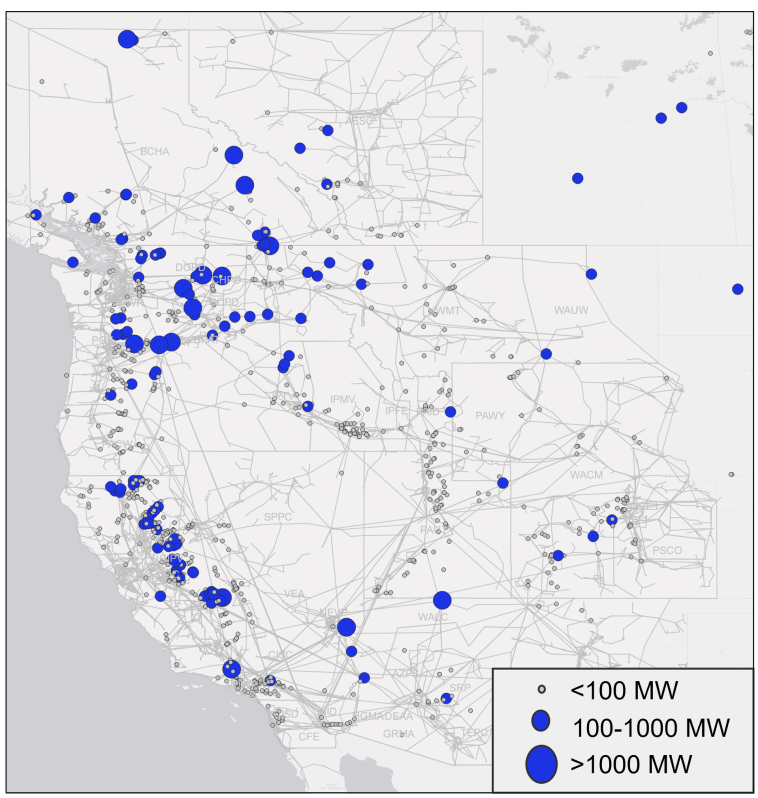

Figure 8. Location of hydropower generators in the WI [29]. A large portion of hydropower resources are located in the northwestern USA and the BC Hydro region in Canada.

Figure 9. Sequence of generator replacement in simulated scenarios

portion, as shown in Fig. 8. Of the ~ 54 GW of hydropower generation in the base case, 39.5 GW is located in the BC, Northwest, and Montana regions. Hence, even with large portions of fossil fuel-based generators replaced by GFM IBRs, the GFM penetration in the northwestern WI never crosses 35% in the simulated scenarios.

In Scenario 1, existing GFL inverters (~ 20 GW) and coal generators (~ 18 GW) were replaced by GFM inverters, resulting in a system-wide GFM penetration of $\sim 23\%$. In Scenario 2, half of natural gas generation (~ 28.3 GW) from each balancing area in the WI was replaced, thereby increasing GFM penetration to $\sim 46\%$. To decide which generators to replace, all natural gas generators in each balancing area were arranged in increasing order of their active power outputs. Then the largest generators making up about half of a given area's natural gas power output were replaced by GFMs. In Scenario 3, the remaining natural gas-based generators were retired in addition to nuclear generators in the WI (~ 5.3 GW). This increased the GFM penetration to $\sim 62\%$. A brief overview of the sequence of generator replacements is shown in Fig. 9. The relative geographic distribution of inverter-based and rotating machines in the created scenarios influence the insights about evolving inter-area oscillations obtained from this work.

2.4 Inter-area Modes in Different Scenarios

As previously discussed, modal properties were estimated by simulating the Chief Joseph brake insertion and then employing Prony analysis to express the system output as a linear combination of damped sinusoids. Prony analysis results are sensitive to the choice of parameters. In this work, the data window to be analyzed was determined through visual inspection; the first two post-disturbance cycles were eliminated, and it was ensured that the data window did not contain any 'flat response' after the oscillations had dissipated. The model order was tuned to achieve a good match between the simulated measurements and the reduced-order Prony model while avoiding overfitting. Studies with brake insertions at different locations will be needed to obtain a comprehensive picture of the modes of the modified system, but the present study has only looked at the oscillations observable from Chief Joseph.

Scenario	Frequency (Hz)	Damping Ratio (%)
1	0.69	15.4
2	0.71	14
3	0.72	14.5

Table 4. Estimates of properties of an inter-area mode around 0.7 Hz observed with increasing GFM penetration in the WI

Modal properties estimated from the base case were first validated against the report published by the WECC [5]. Frequency, DR, and mode shape estimates for the NS modes (NS-A: 0.27 Hz, 14%; NS-B: 0.38 Hz, 11%) approximately matched the findings in the report.

2.4.1 Mode around 0.7 Hz

After GFM penetration was increased following the procedure described in Section 2.3, modal content in the 0.2-0.4 Hz range was no longer visible from post-disturbance data. This is in contrast to the findings from [5], where it was noted that the frequency and DR of the NS modes in the WI change with a system-wide increase in IBR penetration, but the Chief Joseph brake insertion still excites them. This difference may be because- a) the powerflow cases being analyzed are different, and b) this work uses GFM inverters while [5] used GFL IBRs.

Modal content was visible around 0.7 Hz, providing preliminary evidence of the presence of a mode. This frequency is very close to the existing BC modes, although the shape estimates do not exactly match known BC mode behavior, as elaborated later in this section. Modal content in this frequency range was present in all the GFM penetration scenarios simulated in this work, and the estimated mode frequency and DRs are shown in Table 4. The mode appears to be well damped, with DR estimates higher than 10% in all cases, thereby not posing immediate system stability concerns.

Time-domain responses obtained for the simulated cases from two hydropower generators in the region- one in British Columbia, Canada, and the other in the lower Columbia basin, Washington are shown in Fig. 10 and 11. It can be seen that oscillations appear to die out fast, amplitudes appear to decrease, and frequency appears to increase slightly as the inverter penetration is increased.

It is observed that the frequency and DR estimates are consistent in the three simulated scenarios, although a slight increasing trend is observed in mode frequency with an increase in inverter penetration. Previous research corroborates that modal frequencies typically tend to increase as inverter based generation increases in a system [2, 4, 6]. DR estimates do not show a consistent trend, in line with prior observations that inverter locations significantly influence whether mode damping increases or decreases with IBR penetration [3, 4, 6, 8]. (Note that when a mode is highly damped, uncertainty in the estimation of its damping ratio increases.) Further investigation of mode shapes show that as synchronous generators incrementally get replaced by GFM inverters, the geographical spread of this mode decreases and the shape changes. The present work has not investigated what impact, if any, the disconnection of the Alberta-BC 500 kV intertie will have on the 0.7 Hz mode, and this is a direction the authors plan to pursue in future research.

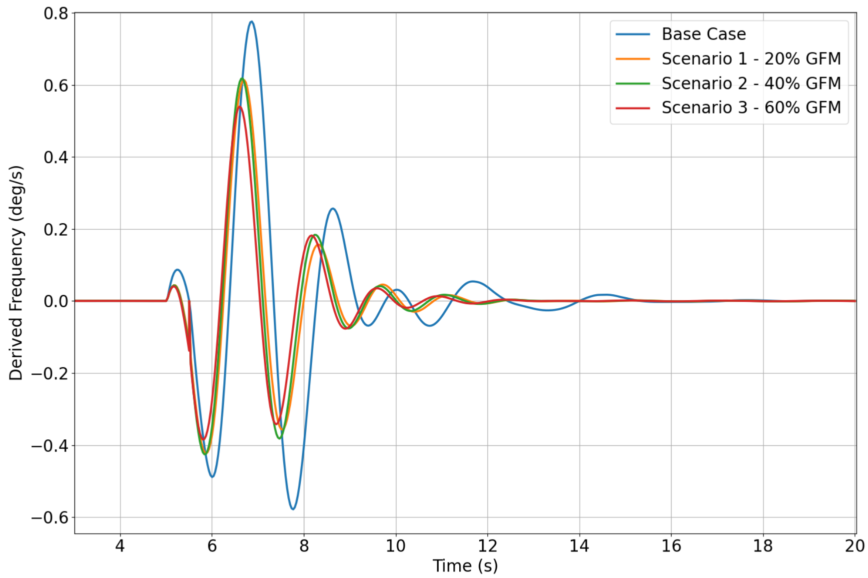

Figure 10. Derived frequency observed at the Kemano bus (British Columbia) in the simulated scenarios

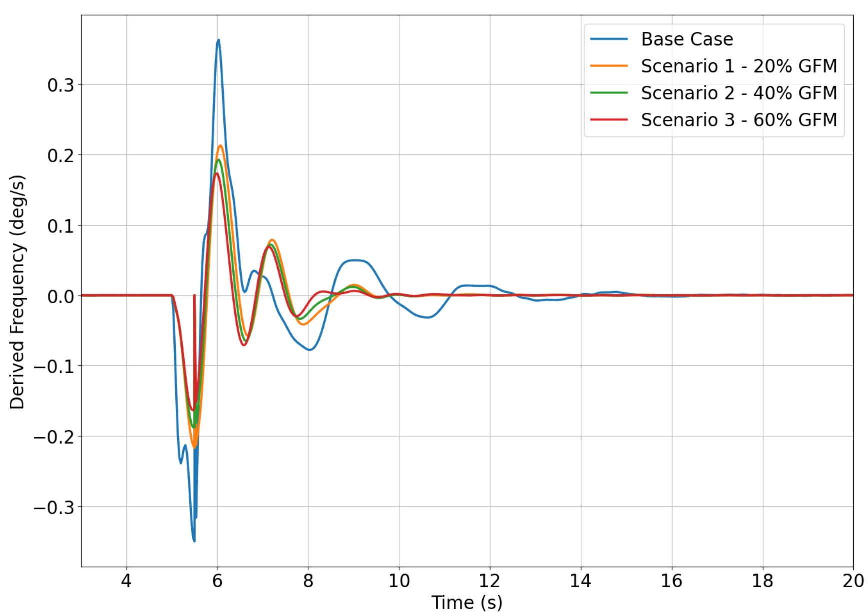

Figure 11. Derived frequency observed at the John Day bus (Washington) in the simulated scenarios

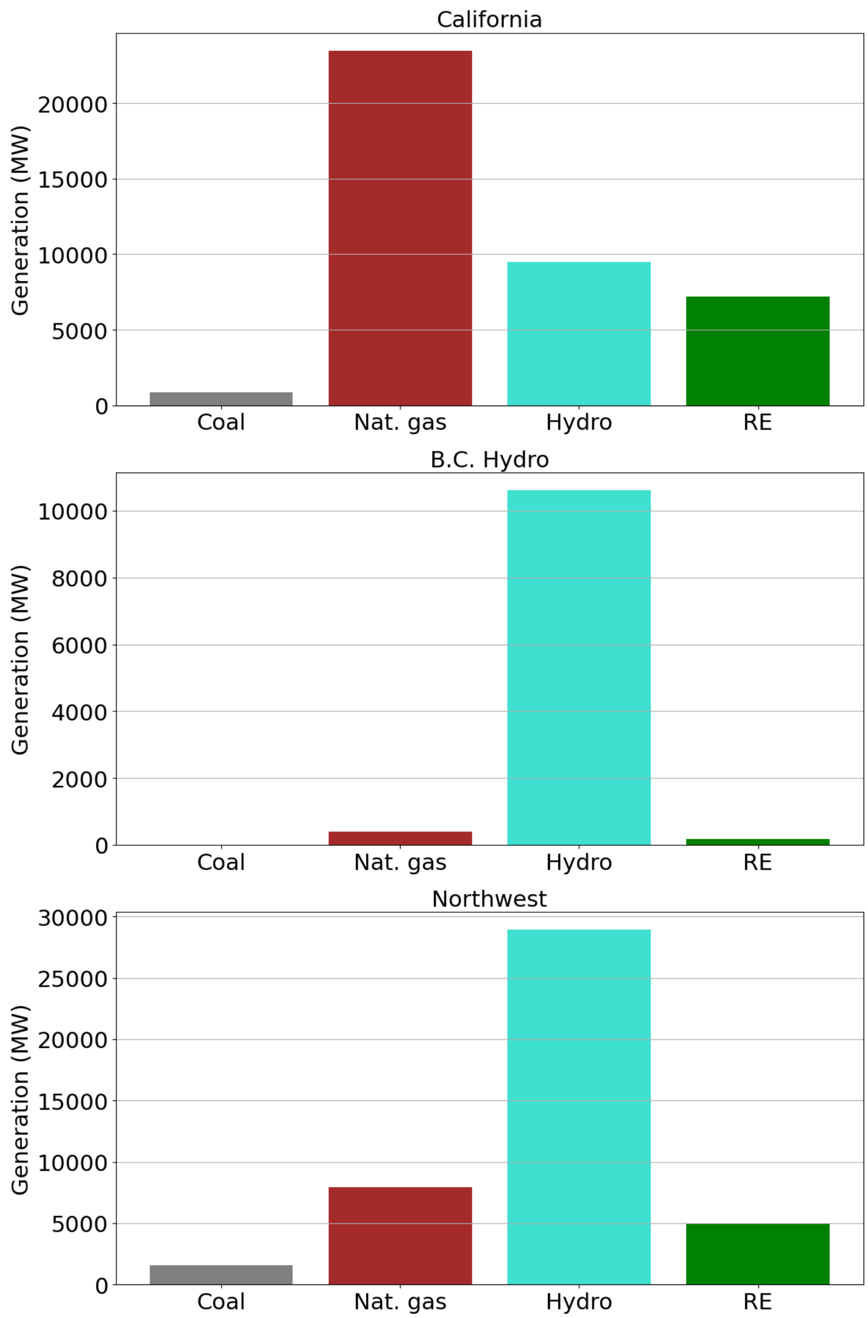

Figure 12. Contribution of different fuels to generation outputs of three areas in the WI (Base case)

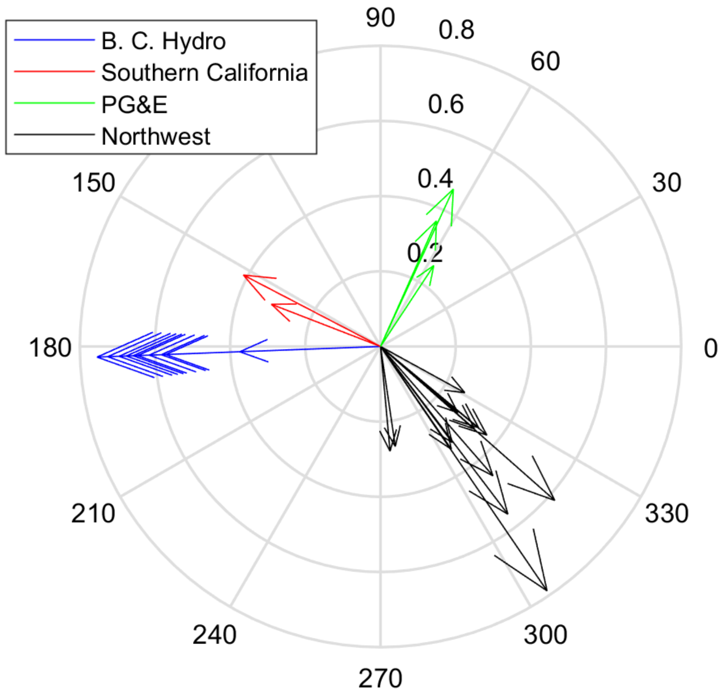

Figure 13. Mode shape estimates: Scenario 1

2.4.2 Resource mix in relevant areas

To support observations from the different scenarios, first examining the fuel mix in areas with significant hydropower generation is useful. Fig. 12 shows the base-case resource mix in the three areas where hydropower makes up a large portion of the generation portfolio and that show participation in the 0.7 Hz mode, namely California, BC Hydro and Northwest.

In California, natural gas is the largest power source in the planning case considered, although significant generation from hydropower and renewable resources is also present. A very small amount of generation comes from coal plants. Hence, behavior differences observed for the region between the base case and Scenario 1 are primarily due to GFL inverters being replaced by GFMs. The replacement of significant natural gas generation in the subsequent scenarios impact inter-area oscillations observed in California.

The major generation source for the BC Hydro region is hydropower. Therefore, the amount of synchronous generation in the region shows little variation across the simulated scenarios. Generators in BC Hydro exhibit high participation in the 0.7 Hz mode.

The Northwest region comprises the states of Washington, Oregon, Idaho and Montana, where several large hydropower plants are present. Some amount of coal, natural gas and inverter-based renewable generation also exist, but participation in the observed 0.7 Hz mode is primarily driven by the energy exchange among hydro-generators.

2.4.3 Mode shape estimates in different scenarios

In Scenario 1, participation in the 0.7 Hz mode is observed from generators in the Northwest, BC and California, as seen from the compass plot in Fig. 13. Compass plots help visualize mode shapes in polar coordinates. Each arrow represents the mode shape of one location; the

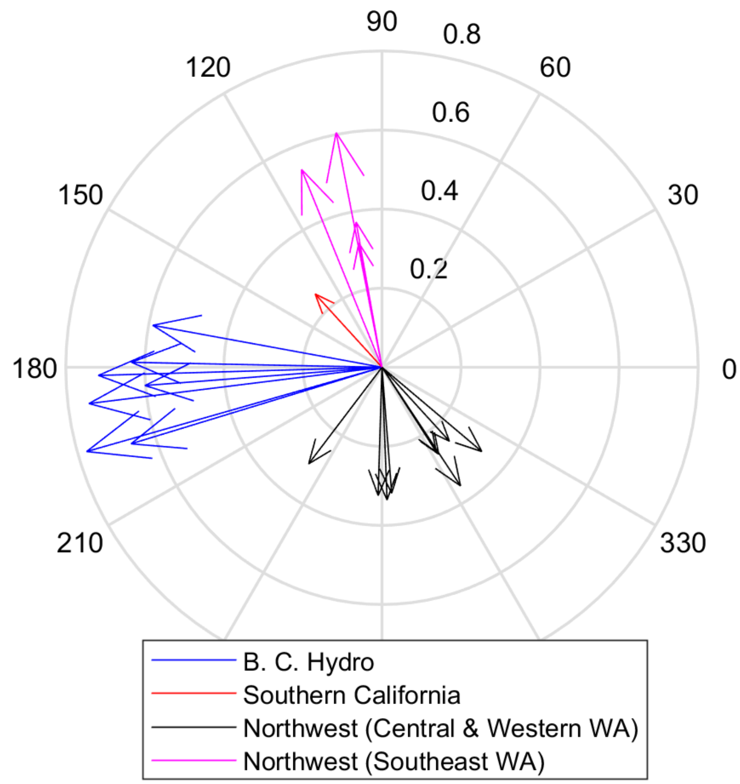

Figure 14. Mode shape estimates: Scenario 2

arrow length is proportional to mode shape amplitude, and direction indicates mode shape angle. The amplitude and angle are expressed in relation to the reference signal, whose shape is $1\angle 0^o$. The reference signal here is the derived frequency (first derivative of voltage angle) from positive sequence voltage angle difference at Wanapum and Kemano buses.

To avoid visual clutter, only locations that had amplitudes greater than 0.2 have been included in the plots shown here. Highest amplitudes are observed in generators in BC Hydro and northwest regions, and the participation in California is from natural gas generators, and small hydropower and geothermal machines. No GFM IBR location had mode shape amplitude estimates higher than 0.2. Because geographically close generators appear to swing together, the mode shape estimates look reasonable.

In Scenario 2, with the retirement of large natural gas generators, participation from California generators in the 0.7 Hz mode decreases significantly, as evident from Fig. 14. This may be explained by the fact that in the base case, California comprised about 23.4 GW of the total 55 GW natural gas generation. Hence, between Scenarios 1 and 2, California sees significant reduction in the number of synchronous machines. It can also be observed that the mode shape angle difference among generators within the Northwest region increases from Scenario 1 to Scenario 2. This shows that the geographic spread of the mode has shrunk, and hydropower generators in central and western Washington are exchanging energy with those in southeastern Washington.

In Scenario 3, with the retirement of further synchronous generators, the geographic spread of the mode reduces again. The highest amplitudes are observed in southeastern Washington, where a large number of high-capacity hydropower plants are concentrated. The large generators in southeast Washington and Idaho appear to swing against those in the central and western

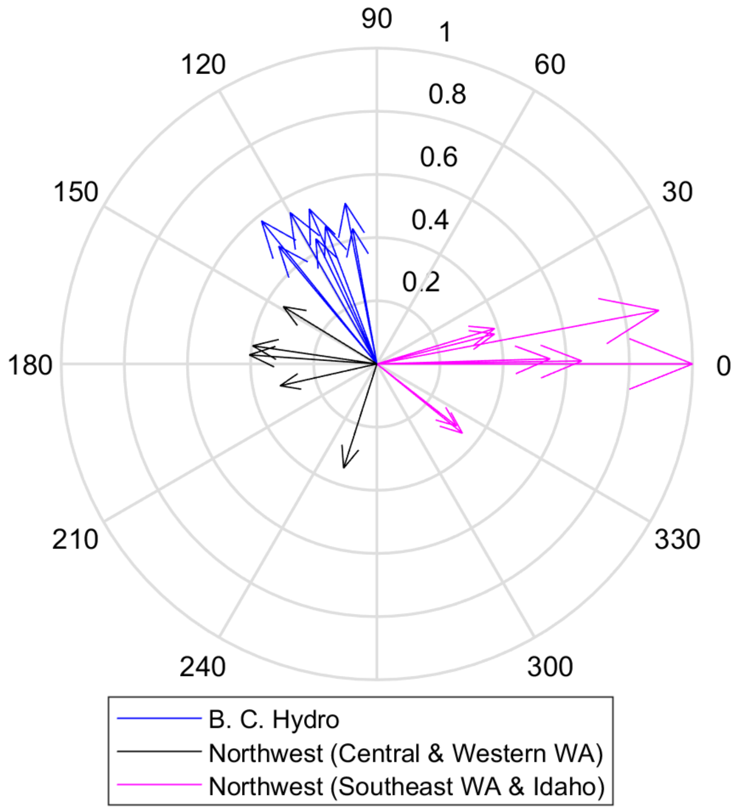

Figure 15. Mode shape estimates: Scenario 3

Washington, as well as the BC Hydro region (Fig. 15). The mode shape is similar to scenario 2, except high participation from California generators is not observed.

To illustrate the changing oscillations in California, Figs 16 and 17 show the oscillatory responses of example generators in the time domain. It can be seen that the oscillations observed at the natural gas bus changes when the synchronous machine in scenario 1 is replaced by a GFM inverter in the remaining scenarios. For the hydropower generator, oscillation amplitudes appear to decrease as GFM penetration increases, in line with the observations described in this section.

It must also be mentioned here that the conclusions from the case-studies are dependent on modeling assumptions. For instance, evidence of poorly tuned inverter controls adversely impacting the damping of oscillatory modes has been documented [30]. However, this work has not examined how improper tuning of GFM control parameters may affect WI modes; the focus is on inter-area oscillations driven by synchronous machines in a GFM inverter-dominated WI.

2.5 Discussion

There exist different hypotheses about how inter-area modes will behave in future inverter-dominated grids. For example, [31] posits that inter-area modes will not disappear in IBR-dominated grids, rather manifest at higher frequencies. On the other hand, [32] says that since the behavior of inverter-dominated grids will no longer be linear around an operating point, the properties of observed oscillations will be highly dependent on contingencies and their locations. The modal properties estimated in this study are preliminary, and dependent on the assumptions

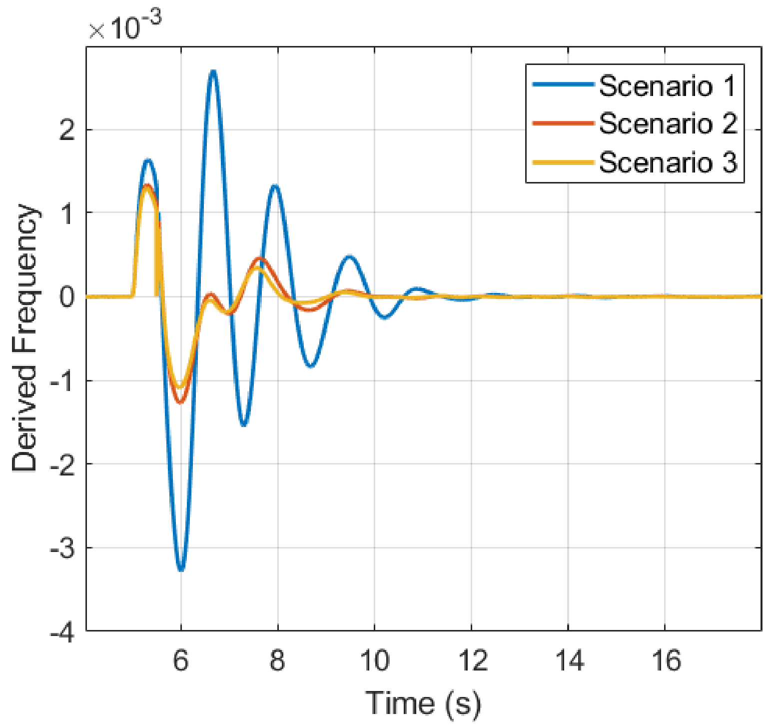

Figure 16. Derived frequency at a California natural gas generator for the three simulated scenarios (replaced by a GFM IBR in Scenarios 2 and 3)

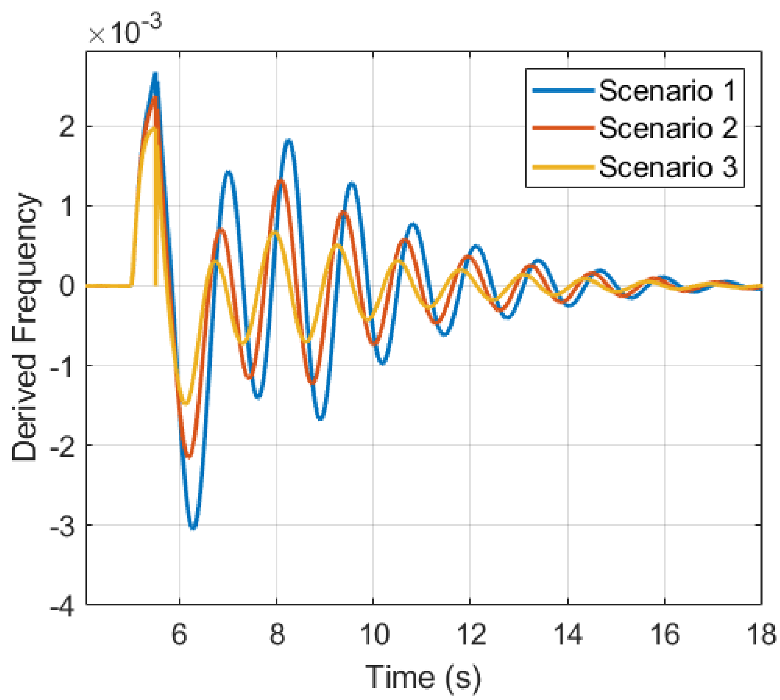

Figure 17. Derived frequency at a California hydropower generator for the three simulated scenarios

about which generators are retired and replaced by GFM IBRs. Moreover, simulations with different power flow models and brake insertions at multiple locations will be necessary for obtaining a complete picture of changing oscillatory modes in the WI.

In any case, as the GFM IBR-penetration scenarios studied in this work are hypothetical, the observation that inter-area oscillation modes will be driven by hydropower generators is a more interesting insight than the exact mode shape estimates obtained. The study indicates that hydropower generator locations that do not show high participation in existing WI modes may end up with increased participation in inter-area oscillations following the reduction of synchronous machines in the system. As regional fuel-mix and IBR control methodologies will dictate future modal properties to a large extent, continuous monitoring will be critical for flagging changes before dramatic transitions in modes occur. Some other actionable insights are listed next.

First, field experience has shown that improperly tuned control parameters of GFM inverters can adversely impact modal properties, especially if the inverters are located in areas with high participation in a mode [30]. Hence, attention must be paid to control parameters of any GFM inverter deployed in northwestern WI. At present, a consensus exists that electromagnetic transient (EMT) studies are necessary for identifying IBR performance issues in areas with high inverter concentration due to low grid strength concerns [33]. Observations from this study indicate that EMT studies may also be necessary in areas with high participation in inter-area modes to ensure that improperly tuned inverter parameters do not exacerbate oscillations caused by transient disturbances.

Second, if modes appear due to the energy exchange among hydropower generators, new interaction paths along which modal energy is transferred may also emerge. Hence, PMU coverage may be necessary for these areas to develop a granular understanding of the WI modal properties.

2.6 Conclusion

In this section, the impact of retiring fossil-fuel-based synchronous generation on the inter-area oscillation modes of the WI has been studied. It is concluded that as inter-area oscillations are primarily driven by the exchange of energy among rotating machines, the synchronous machines remaining in the system and their geographic distribution will dictate the properties of the modes observed. In the WI, as hydropower generation is concentrated in the northwestern portion of the interconnection, retirement of fossil fuel fleets may lead to the emergence of a mode driven by energy exchange among the hydropower generators. Simulations indicate that the mode will be well-damped, thereby not posing immediate threats to system stability. The geographic spread of this mode appears to be limited, and its frequency shows an increasing trend with inverter penetration.

3.0 Observations for the Montana Mode

This chapter describes how the properties and observability of the Montana (MT) mode change, when synchronous machines at the Colstrip power plant are replaced by IBRs. Prior studies indicate that the Costrip plant significantly drives the MT mode in the WI, and hence any change in its characteristics is expected to have a pronounced impact on the MT mode [5]. In the base case, the Colstrip plant consists of two coal-generation units.

To examine how the changing behavior of Colstrip generation units impacts inter-area oscillations, three different cases (see Table 5) were simulated using PSS/E, and a transient disturbance was introduced by simulating a 1200 MW dynamic brake insertion at the Colstrip bus for 0.5 seconds. The resultant transient response was analyzed using the multichannel Prony Analysis technique to estimate MT mode properties. Brake insertion at Colstrip has been shown to excite the MT mode in prior model-based studies [5].

Parameters used for the GFM inverter model (see Table 2) remain the same as the analysis presented in Chapter 2.0. Parameters used for the GFL inverter model (REPC_A+REEC_A+REGC_A) are shown in Table 6 [22–24].

Case	Description
Base case	WECC 2030 heavy winter planning case
Case 1	Both Colstrip units in the base case replaced by GFL inverters
Case 2	Both Colstrip units in the base case replaced by GFM inverters
Case 3	Only Colstrip unit 1 replaced by a GFM inverter

Table 5. Simulated cases to study the MT mode

Parameter	Description	Value
T_{filt}	Voltage reactive power measurement filter time constant	0.02 s
e_{max}	Upper limit on deadband output	0.1 pu
e_{min}	Lower limit on deadband output	-0.1 pu
Q_{max}	Upper limit on output V/Q control	0.6 pu
Q_{min}	Lower limit on output V/Q control	-0.6 pu
P_{max}	Upper limit on power reference	1 pu
P_{min}	Lower limit on power reference	0 pu
D_{dn}	Droop for over-frequency conditions	25 pu
D_{up}	Droop for under-frequency conditions	25 pu
T_{rv}	Voltage filter time constant	0.01s
T_p	Filter time constant for electrical power	0.02s
V_{max}	Max. limit for voltage control	1.1 pu
V_{min}	Min. limit for voltage control	0.86 pu
T_g	Converter time constant	0.0163s
R_{rpwr}	LVPL ramp rate limit	5pu/s

Table 6. Model parameters used for GFL inverters

3.1 Mode Behavior in Different Cases

The frequency and DR estimates obtained for the MT mode in the simulated cases are listed in Table 7. The WECC oscillation analysis report indicates that the frequency of the MT mode varies in the 0.7-0.9 Hz range and DR is typically about 10% [5]. The mode shape is characterized by generation units in Montana swinging against the rest of the system. It is highly observable near the Colstrip and Yellowtail locations, and machines in Washington and Oregon may oscillate either in or out of phase with Montana depending on the operating condition.

In the base case studied in this work, the frequency and DR estimates obtained were on the higher side of the WECC report findings. The mode shape estimates indicated that Washington and Oregon machines were oscillating out of phase with Montana. In Case 1, when the Colstrip units were replaced by GFL inverters, the frequency and DR estimates obtained showed a slight increase and decrease respectively. The decrease in DR may be explained by the removal of the damping contribution of the Colstrip synchronous machines. The mode shape estimates were similar to the base case, indicating that generators in Montana were swinging against the system. However, the oscillation amplitudes observed at the participating generators were lower than the base case, indicating a reduction in MT mode observability/excitability from Colstrip. This behavior is expected, because the Colstrip units are known to be major drivers in the MT mode.

In Case 2, when both Colstrip units are replaced by GFM inverters, the frequency of the MT mode is observed to increase slightly, but the DR shows significant increase. As the oscillations damp down very fast, the data window available to obtain estimates using Prony analysis is quite short. This may impact the estimation accuracy of mode frequency and DR, but the observation

Case	Frequency (Hz)	Damping Ratio (%)
Base Case	0.902	11.71
Case 1	0.963	9.81
Case 2	0.986	18.37
Case 3	0.963	15.18

Table 7. Montana mode properties estimated in different cases

that oscillations die down faster than the other cases checked indicates that the mode is better damped in this scenario. The dominance of MT mode is reduced in the system's transient response. However, synchronous machines in Montana are still observed to swing in phase against machines in other parts of the interconnection. The voltage angle variation at Colstrip unit 1 under different configurations (synchronous machine, GFL inverter, GFM inverter) in different cases is shown in Fig. 18.

In Case 3, only Colstrip unit 1 is replaced by a GFM inverter, while Colstrip unit 2 is represented as a synchronous generator. Both the frequency and DR estimates obtained are higher than the base case but lower than Case 2. Derived frequency (first derivative of voltage angle) variation at the two Colstrip units in the Case 3 simulation is shown in Fig. 20. Note that the voltage angle variation is smoother in Colstrip unit 1 (GFM inverter), while oscillations are visible in the response of Colstrip unit 2 (synchronous machine).

That synchronous machines in Montana still swing against the system close to the 0.9 Hz frequency range is visible from the time-domain response of the Yellowtail hydro-unit in south-central Montana, as shown in Fig. 19. The figure shows that as the Colstrip units are replaced by IBRs, the oscillation frequencies shift slightly and amplitudes are reduced. As the IBRs at the Colstrip location no longer participate in oscillations in the electromechanical range, this behavior is expected.

3.2 Conclusion

From the simulation results described in this chapter, it may be concluded that any change in the configuration of Colstrip power plants will have a pronounced impact on the characteristics of the Montana mode in the WI. If the synchronous machines are replaced by IBRs, then the IBR control methodology used will dictate how the mode characteristics change. Generators in Montana may still continue to swing together around the 0.9 Hz frequency, but mode observability across the system may be reduced.

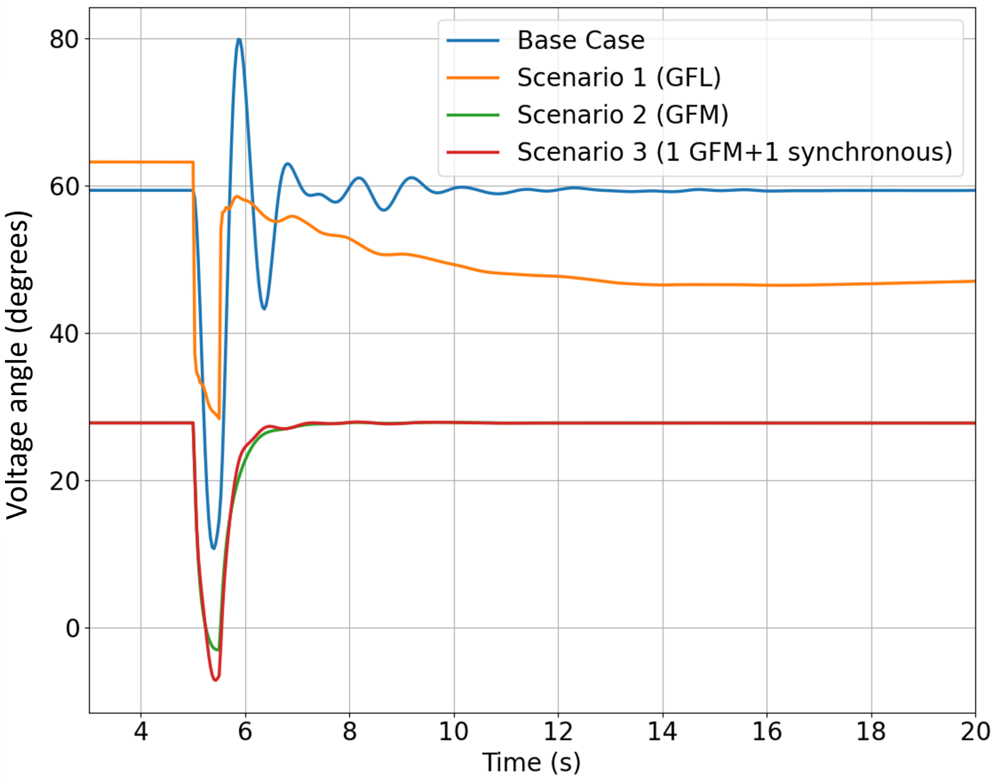

Figure 18. Voltage angle at Colstrip 1 at different configurations. Dotted black lines indicate the dynamic brake insertion period.

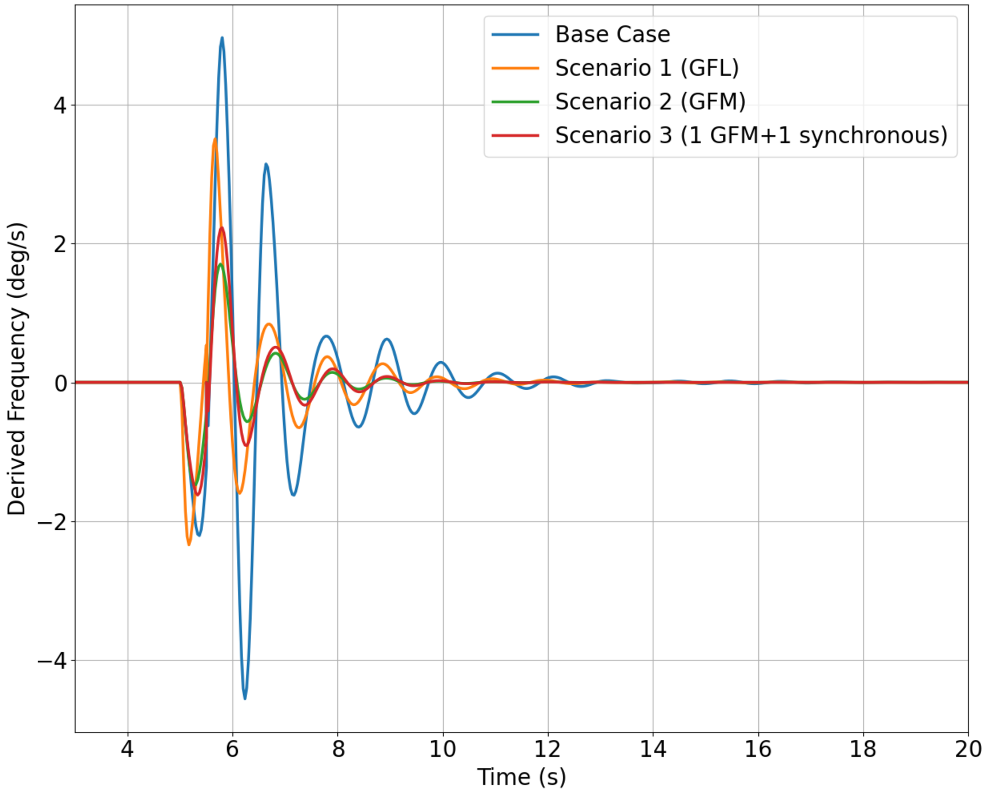

Figure 19. Derived frequency variation at the Yellowtail unit, a hydropower generator in Montana, in the simulated cases

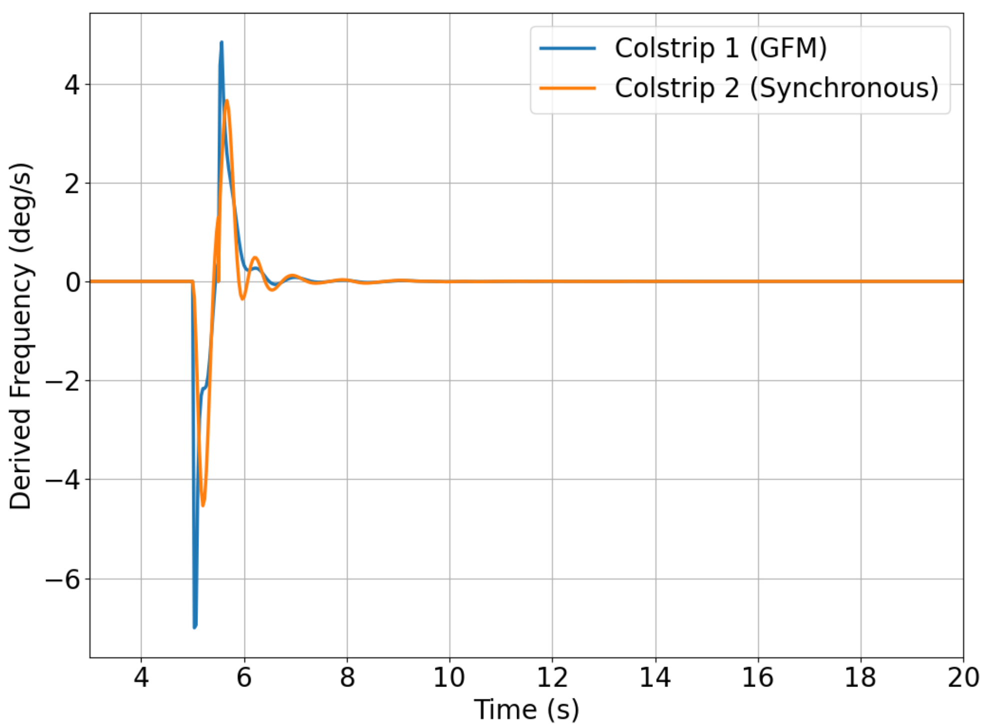

Figure 20. Derived frequency variation at the two Colstrip units in Case 3

4.0 Further Work

This report describes preliminary work performed to analyze how inter-area modes in the WI may change if synchronous machines are replaced by GFM IBRs. To obtain a more comprehensive understanding of how new resources may change oscillation characteristics in the interconnections, the following avenues will be pursued-

- Dynamic brake insertion at different locations in the WI to observe modal properties under different GFM IBR penetrations.
- Comparison of system oscillation characteristics when the GFM inverters in the studied scenarios are replaced by GFL inverters. This will allow granular understanding of the impact of inverter control strategies on system transient response.
- Studying the impact of varying GFL and GFM penetrations.
- Investigating the impact of varying inverter parameters on the transient response of large interconnections under high IBR-penetration scenarios.

Moreover, the prepared power flow cases and dynamic simulation models will also be used in the macro-grid (a grid model representing both WECC and EI systems) modelling enabled by the HVDC user defined module developed by another DOE-funded project.

5.0 References

[1] NERC Synchronized Measurement Working Group, “Recommended oscillation analysis for monitoring and mitigation reference document,” Nov. 2021.

[2] S. You, G. Kou, Y. Liu, X. Zhang, Y. Cui, M. J. Till, W. Yao, and Y. Liu, “Impact of high PV penetration on the inter-area oscillations in the US Eastern Interconnection,” *IEEE Access*, vol. 5, pp. 4361–4369, 2017.

[3] U. Agrawal, R. Huang, X. Fan, and Z. Huang, “Analysis of the Impact of the Increasing Inverter-based Resources on Inter-area Modes of the U.S. Eastern Interconnection,” May 2022.

[4] R. Elliott, R. Byrne, A. Ellis, and L. Grant, “Impact of increased photovoltaic generation on inter-area oscillations in the Western North American power system,” in *IEEE PES General Meeting*, (National Harbor, MD), 2014.

[5] Western Interconnection Modes Review Group, “Modes of inter-area power oscillations in the Western Interconnection,” 2021.

[6] T. Ahmad, N. Zhou, J. Follum, R. Huang, S. Wang, U. Agrawal, P. Etingov, and Z. Huang, “Estimation of the correlation between oscillation modes and operating conditions using quantile regression: A measurement-based approach,” in *52nd North American Power Symposium (NAPS)*, pp. 1–6, IEEE, 2021.

[7] “WECC wide-area oscillation assessment and trending study report,” Tech. Rep. PNNL-33651, PNNL, Oct. 2022.

[8] T. Xu, W. Jang, and T. J. Overbye, “Location-dependent impacts of resource inertia on power system oscillations,” in *51st Hawaii International Conference on System Sciences (HICSS 2018)*, January 2018.

[9] Y. Cheng, L. Fan, J. Rose, S.-H. Huang, J. Schmall, X. Wang, X. Xie, J. Shair, J. R. Ramamurthy, N. Modi, C. Li, C. Wang, S. Shah, B. Pal, Z. Miao, A. Isaacs, J. Mahseredjian, and J. Zhou, “Real-world subsynchronous oscillation events in power grids with high penetrations of inverter-based resources,” *IEEE Transactions on Power Systems*, vol. 38, no. 1, pp. 316–330, 2023.

[10] S. Dong, B. Wang, J. Tan, C. J. Kruse, B. W. Rockwell, and A. Hoke, “Analysis of november 21, 2021, kaua‘i island power system 18-20 hz oscillations,” 2023.

[11] R. H. Lasseter, Z. Chen, and D. Pattabiraman, “Grid-forming inverters: A critical asset for the power grid,” *IEEE Journal of Emerging and Selected Topics in Power Electronics*, vol. 8, no. 2, pp. 925–935, 2020.

[12] W. Du, Y. Liu, F. K. Tuffner, R. Huang, and Z. Huang, “Model specification of droop-controlled, grid-forming inverters (GFMDRP_A),” Tech. Rep. PNNL-32278, Pacific Northwest National Laboratory, Dec. 2021.

[13] S. Biswas, Q. Nguyen, X. Lyu, X. Fan, and Z. Huang, “Evaluating the impact of retiring synchronous fossil fuel generators on inter-area oscillations in the U.S. Western Interconnection,” in *57th Hawaii International Conference on System Sciences (HICSS 2024)*, January 2024.

[14] D. Kosterev, C. Taylor, and W. Mittelstadt, “Model validation for the august 10, 1996 WSCC system outage,” *IEEE Transactions on Power Systems*, vol. 14, no. 3, pp. 967–979, 1999.

[15] D. J. Trudnowski, J. W. Pierre, N. Zhou, J. F. Hauer, and M. Parashar, "Performance of three mode-meter block-processing algorithms for automated dynamic stability assessment," *IEEE Transactions on Power Systems*, vol. 23, no. 2, pp. 680–690, 2008.

[16] J. D. Follum, N. Nayak, and J. H. Eto, "Online tracking of two dominant inter-area modes of oscillation in the eastern interconnection," in *56th Hawaii International Conference on System Sciences (HICSS 2023)*, January 2023.

[17] D. Trudnowski, J. Johnson, and J. Hauer, "Making prony analysis more accurate using multiple signals," *IEEE Transactions on Power Systems*, vol. 14, no. 1, pp. 226–231, 1999.

[18] G. Liu, J. Quintero, and V. M. Venkatasubramanian, "Oscillation monitoring system based on wide area synchrophasors in power systems," in *2007 iREP Symposium - Bulk Power System Dynamics and Control - VII. Revitalizing Operational Reliability*, pp. 1–13, 2007.

[19] L. Wang and A. Semlyen, "Application of sparse eigenvalue techniques to the small signal stability analysis of large power systems," *IEEE Transactions on Power Systems*, vol. 5, no. 2, pp. 635–642, 1990.

[20] Powertech Labs, "SSAT small signal analysis tool."

[21] W. Trinh, K. Shetye, I. Idehen, and T. Overbye, "Iterative matrix pencil method for power system modal analysis," in *52nd Hawaii International Conference on System Sciences (HICSS 2019)*, January 2019.

[22] "Model REPC_A renewable energy plant control." `https://www.powerworld.com/WebHelp/Content/TransientModels_HTML/Plant%20Controller%20REPC_A.htm`.

[23] "Model REEC_A renewable energy electrical control model." `https://www.powerworld.com/WebHelp/Content/TransientModels_HTML/Machine%20Model%20REGC_A.htm`.

[24] "Model REGC_A renewable energy converter/generator." `https://www.powerworld.com/WebHelp/Content/TransientModels_HTML/Machine%20Model%20REGC_A.htm`.

[25] W. Du, Q. Nguyen, Y. Liu, and S. M. Mohiuddin, "A current limiting control strategy for single-loop droop-controlled grid-forming inverters under balanced and unbalanced faults," in *2022 IEEE Energy Conversion Congress and Exposition (ECCE)*, pp. 1–7, IEEE, 2022.

[26] WECC, "WECC anchor dataset (ADS)." `https://www.wecc.org/ReliabilityModeling/Pages/AnchorDataSet.aspx`.

[27] M. L. Shelton, P. Winkelman, W. A. Mittelstadt, and W. Bellerby, "Bonneville power administration 1400-MW braking resistor," *IEEE Transactions on Power Apparatus and Systems*, vol. 94, pp. 602–611, 1975.

[28] X. Fan, W. Du, Q. Nguyen, M. Elizondo, S. Wang, J. Follum, S. Kincic, H. Huang, Y. Chen, S. Biswas, X. Lyu, K. Chatterjee, S. Nekkalapu, H. Mahmood, N. Zhou, D. Trudnowski, and B. Barazesh, "Automated creation of varying penetrations of GFM IBRs for Western Interconnection wide-area oscillation study," in *WECC MVS Meeting*, (Vancouver, BC), May 2023.

[29] Homeland Infrastructure Foundation-Level Data (HIFLD), "Power plants." `https://hifld-geoplatform.opendata.arcgis.com/datasets/power-plants-2/explore`. Accessed: 2023-06-12.

[30] E. Farahani, P. Mayer, J. Tan, F. Spescha, and M. Gordon, "Oscillatory interaction between large scale IBR and synchronous generators in the NEM," *CIGRE Science & Engineering*, Mar. 2023.

[31] M. Zhang, Z. Miao, L. Fan, and S. Shah, "Data-driven interarea oscillation analysis for a 100% IBR-penetrated power grid," *IEEE Open Access Journal of Power and Energy*, vol. 10, pp. 93–103, 2022.

[32] T. J. Overbye and S. Kunkolienkar, "On the existence of distinct inter-area electromechanical modes in North American electric grids," 2023.

[33] NERC, "Reliability guideline electromagnetic transient modeling for BPS connected inverter-based resources— recommended model requirements and verification practices," Mar. 2023.

Pacific Northwest
National Laboratory

902 Battelle Boulevard
P.O. Box 999
Richland, WA 99352
1-888-375-PNNL (7665)

www.pnnl.gov